

Article

Novel *N*-Substituted 2-(2-(Adamantan-1-yl)-1*H*-Indol-3-yl)-2-Oxoacetamide Derivatives: Synthesis and Biological Evaluation

Hong-Yu Hu [†], Xu-Dong Yu [†], Fei Wang, Chun-Rong Lin, Jin-Zhang Zeng, Ying-Kun Qiu, Mei-Juan Fang ^{*} and Zhen Wu ^{*}

School of Pharmaceutical Sciences and the Key Laboratory for Chemical Biology of Fujian Province, Xiamen University, South Xiang-An Road, Xiamen 361102, China; huhongyu22@126.com (H.-Y.H.); yuxudong91@163.com (X.-D.Y.); tjdxwangfei@163.com (F.W.); reyai@163.com (C.-R.L.); jzzeng@xmu.edu.cn (J.-Z.Z.); qyk@xmu.edu.cn (Y.-K.Q.)

^{*} Correspondence: fangmj@xmu.edu.cn (M.-J.F.); wuzhen@xmu.edu.cn (Z.W.);
Tel./Fax: +86-592-218-9868 (M.-J.F. & Z.W.)

[†] These authors contributed equally to this work.

Academic Editor: Jean Jacques Vanden Eynde

Received: 7 March 2016; Accepted: 16 April 2016; Published: 5 May 2016

Abstract: In this study, a series of novel *N*-substituted 2-(2-(adamantan-1-yl)-1*H*-indol-3-yl)-2-oxoacetamide derivatives were synthesized, and evaluated for their cytotoxicity in human cell lines including Hela (cervical cancer), MCF7 (breast cancer) and HepG2 (liver cancer). Several compounds were found to have potent anti-proliferative activity against those human cancer cell lines and compound **5r** showed the most potent biological activity against HepG2 cells with an IC₅₀ value of 10.56 ± 1.14 μM. In addition, bioassays showed that compound **5r** induced time-dependent and dose-dependent cleavage of poly ADP-ribose polymerase (PARP), and also induced a dose-dependent increase in caspase-3 and caspase-8 activity, but had little effect on caspase-9 protease activity in HepG2 cells. These results provide evidence that **5r**-induced apoptosis in HepG2 cell is caspase-8-dependent.

Keywords: 2-(2-(adamantan-1-yl)-1*H*-indol-3-yl)-2-oxoacetamide derivatives; poly ADP-ribose polymerase (PARP); caspase-8; apoptosis

1. Introduction

Despite continued research efforts, cancer remains one of the biggest threats to human health, and it was estimated to be responsible for 15% of all global deaths in 2010 [1]. Current treatment for tumors generally involves surgical resection (if possible), followed by radiotherapy and chemotherapy, with the most common chemotherapies, according to Cancer Research UK, being temozolomide, procarbazine, carmustine, lomustine and vincristine [2–5]. However these drugs alone simply aren't sufficient for long-term treatment because of the rapid chemoresistance developed by many cancers [6]. Multidrug resistance (MDR) is a major obstacle to successful cancer treatment [7,8]. This has driven the development of a variety of new anticancer agents with more potent, high specific and low cytotoxic properties [9].

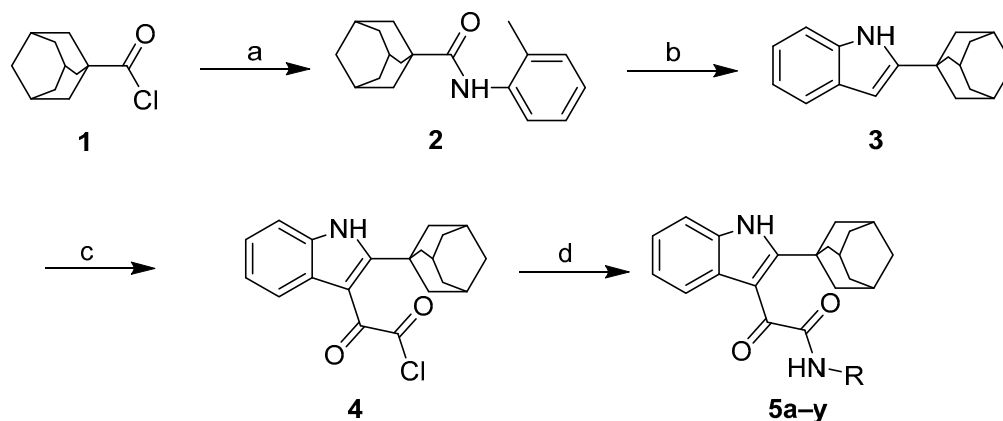
The indole moiety has been described as a privileged structure as it appears extensively in many unrelated areas of biology and medicine, and depending on the substituents, can have a diverse range of effects [10]. The indole ring system as one of the most ubiquitous heterocycles in Nature, and has been becoming an important structural component in many pharmaceutical agents, such as antidepressant [11], anticonvulsant [12], antifungal [13], antiviral [14] and anti-inflammatory [15], and particularly new antitumor agents [16–19]. Indole-3-glyoxylamide compounds, as a new class of

indole derivatives which have anti-tumor [20–22], anti-viral [23], anti-bacterial [24,25], anti-HIV [26], adenosine regulating receptor function [27] and other biological activities, have become one of the most important chemical entities in the field of pharmaceutical research. Thus, we synthesized a novel class of *N*-substituted 2-(2-(adamantan-1-yl)-1*H*-indol-3-yl)-2-oxoacetamide derivatives and evaluated their *in vitro* anti-proliferative activity against human breast (MCF7), cervical (Hela) and liver (HepG2) cancer cells. To explain the molecular mechanisms mediating the induction of apoptosis by this class of compounds, the activation of caspase-3, caspase-8 and caspase-9 was further examined using a caspase activity assay kit in HepG2 cells after treatment with compound **5r**.

2. Results and Discussion

2.1. Chemistry

The preparation of the *N*-substituted 2-(2-(adamantan-1-yl)-1*H*-indol-3-yl)-2-oxoacetamide derivatives **5a–y** is outlined in Scheme 1. First, we synthesized 2-adamantane-1*H*-indol-5-amine (**3**). The general chemistry used in the synthesis of **3** was adapted from reported previously methods [28,29]. Briefly, treatment of adamantane-1-carbonyl chloride (**1**) with *o*-Toluidine resulted in *N*-*o*-tolylcycloadamantanecarboxamide (**2**), followed by dropwise addition of 1.4 or 1.6 M *n*-BuLi in hexane to get the compound **3**. Then the intermediate 2-(2-(adamantan-1-yl)-1*H*-indol-3-yl)-2-oxoacetyl chloride (**4**) was easily formed by the reaction of **3** and oxalyl chloride in anhydrous diethyl ether. Finally, the reaction of compound **4** with various substituted amines in toluene at 60 °C for 4 h afforded the title compounds **5a–y**. The structures of all the target compounds were confirmed by their spectral data (HRMS, ¹H-NMR and ¹³C-NMR).

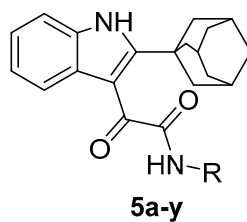


Scheme 1. Synthesis of *N*-substituted 2-(2-(adamantan-1-yl)-1*H*-indol-3-yl)-2-oxoacetamide. *Reagents and conditions:* (a) toluene, *o*-toluidine, K₂CO₃, r.t., 4 h; (b) *n*-BuLi, THF, 0 °C, N₂, 3 h; (c) ether, oxalyl chloride, 0 °C, 2 h; (d) toluene, *o*-toluidine, K₂CO₃, r.t., 4 h.

2.2. Biological Evaluation

2.2.1. Cytotoxicity in Human Tumor Cell Lines

All synthesized compounds were evaluated for their *in vitro* anti-proliferative activity against three human cancer cell lines: MCF-7 (breast cancer cells), Hela (cervical cancer cells), HepG2 (liver cancer cells). The concentration required for 50% inhibition of cell viability (IC₅₀) was calculated and the results are given in Table 1. Most compounds showed a moderate anti-proliferative activity against all tested cell lines, whereas compounds **5a**, **5b**, **5e** and **5j** exhibited relatively weak activity against one or all tested cell lines, with IC₅₀ values over 100 μM. On the other hand, **5i**, **5p**, **5r** and **5y** exhibited good cytotoxicity against HepG2, whereas compound **5f**, with an IC₅₀ value of 17.65 ± 1.54 μM, was more active against Hela.

Table 1. Inhibition of humor cancer cell lines (Hela, MCF7 and HepG2) by *N*-substituted 2-(2-(adamantan-1-yl)-1*H*-indol-3-yl)-2-oxoacetamide derivatives.

Compound	Structure	MTT (IC ₅₀ , μM)		
	R	Hela	MCF7	HepG2
5a		>100	>100	>100
5b		62.13 ± 3.45	>100	56.46 ± 2.71
5c		43.21 ± 1.67	46.12 ± 2.15	37.87 ± 0.87
5d		42.14 ± 2.61	46.19 ± 1.34	35.67 ± 1.69
5e		>100	>100	61.12 ± 2.54
5f		17.65 ± 1.54	24.24 ± 1.09	20.89 ± 0.87
5g		42.12 ± 1.94	40.67 ± 1.48	35.65 ± 1.02
5h		41.21 ± 1.54	38.91 ± 1.04	25.69 ± 2.01
5i		28.23 ± 1.16	26.11 ± 0.98	25.14 ± 0.61
5j		>100	29.25 ± 1.90	21.34 ± 0.98
5k		45.61 ± 1.67	36.15 ± 1.23	36.75 ± 1.85
5l		65.43 ± 1.15	68.21 ± 2.78	43.21 ± 1.45
5m		85.34 ± 1.54	76.34 ± 1.25	57.17 ± 2.15
5n		54.32 ± 1.15	41.24 ± 1.12	40.13 ± 2.54

Table 1. Cont.

Compound	Structure	MTT (IC ₅₀ , μM)		
	R	Hela	MCF7	HepG2
5o		35.13 ± 1.98	45.13 ± 2.32	43.12 ± 2.32
5p		40.14 ± 1.56	37.45 ± 0.67	22.24 ± 1.68
5q		36.56 ± 1.12	35.65 ± 1.41	38.65 ± 1.63
5r		16.12 ± 1.54	12.54 ± 1.15	10.56 ± 1.14
5s		34.35 ± 1.45	45.83 ± 2.41	35.67 ± 1.14
5t		37.32 ± 1.78	49.32 ± 2.16	36.76 ± 0.79
5u		47.32 ± 1.78	56.14 ± 2.38	42.15 ± 2.53
5v		78.34 ± 0.56	56.34 ± 1.56	41.22 ± 2.19
5w		32.15 ± 2.21	43.12 ± 2.10	46.14 ± 1.45
5x		42.15 ± 2.23	53.12 ± 2.16	41.14 ± 1.92
5y		31.47 ± 1.24	29.25 ± 1.90	21.34 ± 0.98

Interestingly, compound **5a** with a *N*-cyclopropyl group exhibited the lowest cytotoxic activity against these three cancer lines, with IC₅₀ values of over 100 μM, however introduction of single ring aryl group at the *N*-position such as in compounds **5c**, **5d** and **5f** caused an increase in cytotoxic activity, and among them compound **5f** with a *N*-benzene substituent had the strongest cytotoxic activity against the Hela cell line, with an IC₅₀ value of 17.65 ± 1.54 μM. These data suggested the presence of alkyl ring at the *N'*-position had an important relationship with anti-proliferative activity. To investigate the impact of the substituents on the *N*-phenyl ring, halogen (F, Cl, Br or I),

methyl (CH₃), trifluoromethyl (CF₃), methoxy (OCH₃), cyano (CN), nitro (NO₂) and/or methoxy formyl (COOCH₃) was introduced (compounds **5g–u**). Substitution at the *N*-phenyl ring was unhelpful, except for compound **5r** with *m*-Cl and *p*-F on the *N*-phenyl ring as shown in Table 1. In addition, replacement of phenyl with pyridyl (**5v** and **5w**), pyrimidine (**5x**) or isoxazole (**5y**) resulted in similar cellular anti-proliferative activity and the introduction of a fused aromatic ring group (compound **5e**) or alkyl group (**5b**) between nitrogen atom and phenyl group was generally unfavorable for anti-proliferative properties.

Based on data collected from three independent experiments, compound **5r** showed the most cytotoxic activity against Hela, MCF-7 and HepG2 cell lines with IC₅₀ values of 16.12 ± 1.54, 12.54 ± 1.15 and 10.56 ± 1.14 μM, respectively, so we used compound **5r** for further biological activity studies.

2.2.2. Growth Inhibitory Activity of **5r** in HepG2

As cell proliferation depends on cell division which is regulated by the cell cycle, absence of normal cell-cycle control is a hallmark of cancer [30]. Cell cycle-related proteins have been as the therapeutic targets against cancer and lots of small molecules were developed as potent antitumor agents, such as microtubule-targeting agents, and cyclin-dependent kinases, aurora kinases and polo-like kinases inhibitors [31–34]. The present study sought to determine how compound **5r** inhibited HepG2 cell growth. Microscopic analysis indicated that the colonies of HepG2 cells decreased after compound **5r** treatment in a dose dependent manner, compared to the control group (Figure 1A). Furthermore, flow cytometry was performed to examine cell cycle inhibition after 12 h of compound **5r** treatment. The results revealed a significant accumulation of cell-cycle arrest, with a decrease in G0/G1 phase and an increase in G2/M phase arrest at 12 h, indicating that inhibitory activity of compound **5r** was associated with disruption of cell cycle (Figure 1B). Meanwhile, the effects of compound **5r** on colony-formation and cell-cycle distribution in Hela and MCF-7 cells were also examined (see Supplementary Materials).

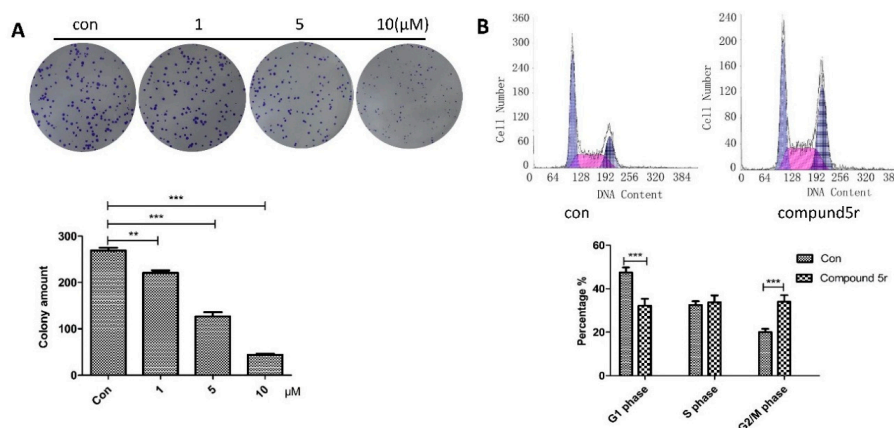


Figure 1. Effects of compound **5r** on colony-formation and cell-cycle distribution in HepG2 cells. (A) Compound **5r** inhibits the colony-forming activity of HepG2 cells. Cells were grown in 6-well plates for 6 days and treated with compound **5r** (1, 5 and 10 μM). Colonies of HepG2 cells decreased after compound **5r** treatment in a dose dependent manner (** $p < 0.01$ and *** $p < 0.001$ compared with the control, *t*-test); (B) A flow cytometry assay was performed to examine cell cycle arrest. HepG2 cells were treated with 10 μM compound **5r** for 12 h. Compound **5r** reduced a significant accumulation of cell-cycle arrest (*** $p < 0.001$ compared with the control, *t*-test).

2.2.3. Inducing Apoptosis in HepG2 Cells

Apoptosis, as a fundamental biological process, plays an important role in cell growth, development and tissue homeostasis [35–37]. Deregulation in apoptotic cell contributes to many diseases, including cancer, neurodegenerative disorders and cardiovascular diseases [38,39]. Apoptosis

can be further characterized as cell death accompanied by the activation of a unique family of cysteine-dependent specific proteases called caspases [40]. Two major signaling pathways induce apoptotic cell death: the mitochondrial pathway and the death receptor pathway [41]. The former relies on mitochondrial depolarization and permeability increase in response to a variety of cellular stresses, including DNA damage, growth factor deprivation, ER stress, thus resulting in the release of cytochrome C, then initiating formation of an APAF-1/caspase-9 complex and activation of downstream executionary caspases, including caspase-3, caspase-6, and caspase-7, and finally leading to cell death [42,43]. The second pathway is activated predominantly by the binding of death receptor ligands, including tumor necrosis factor- α (TNF- α), fas ligand (CD95) and tumor necrosis factor-related apoptosis inducing ligand (TRAIL) to their respective death receptors, then initiating the assembly of large macromolecular complexes that recruit and activate caspase-8, which further cleave and activate caspase-3 for apoptosis [44]. In our work, it was demonstrated that compound **5r** could induce poly ADP-ribose polymerase (PARP) cleavage, which served as a marker of cells undergoing apoptosis, in a time- and dose-dependent manner (Figure 2A,B).

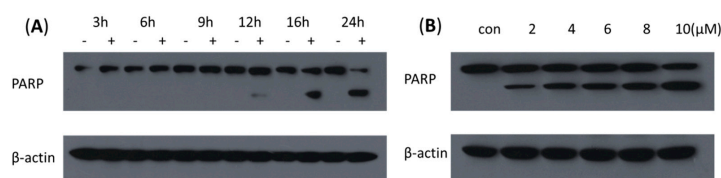


Figure 2. Apoptosis induction by compound **5r** in HepG2. Western blot analysis of PARP in HepG2 cells treated with 10 μ M compound **5r** for different periods of time (0, 3, 6, 9, 12, 16 and 24 h) (A); and different concentration of compound **5r** (2, 4, 6, 8 and 10 μ M) for 24 h (B).

The PARP is one of the important targets of caspase-3, which is also downstream of caspase-8 and caspase-9 [45]. Therefore, the activation of caspase-3, caspase-8 and caspase-9 was examined in HepG2 cells using a caspase activity assay kit after treatment with compound **5r**. It was shown that compound **5r** significantly stimulated caspase-3 and caspase-8 protease activities in HepG2 cells, yet had little effect on caspase-9 protease activity (Figure 3). The results suggested that compound **5r** resulted in the caspases-3 activation and PARP cleavage by activating caspase-8, finally leading to cell death.

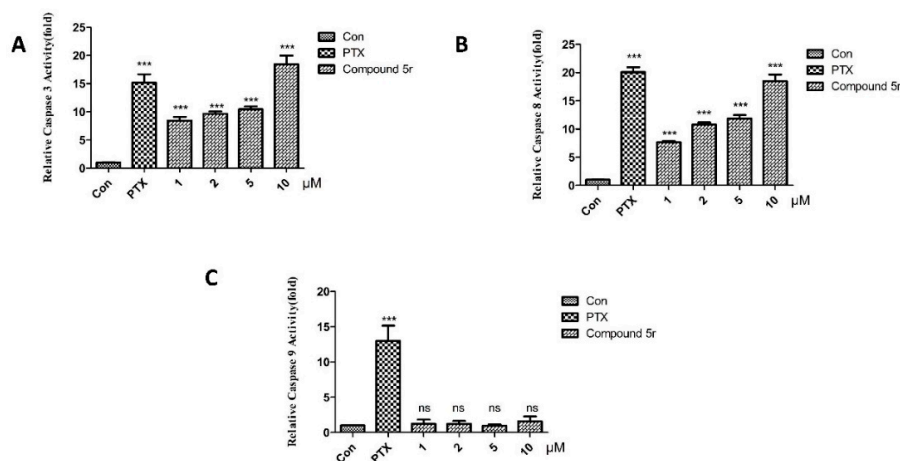


Figure 3. Induction of caspase-3, caspase-8 and caspase-9 by compound **5r** in HepG2. Cells were treated with different concentration of compound **5r** (1, 2, 5 and 10 μ M) and analyzed by caspase-3 (A); caspase-8 (B) and caspase-9 (C) activity assay kit. As a positive control, HepG2 cells were treated with (PTX, 1 μ M) and analyze. Compound **5r** significantly stimulated caspase-3 and caspase-8 protease activities in HepG2 cells, yet had little effect on caspase-9 protease activity (** $p < 0.001$ and ns $p > 0.05$ compared with the control, t -test).

3. Materials and Methods

3.1. General Information

All reagents were commercially available and used without further purification unless otherwise indicated. Reaction mixtures were magnetically stirred and monitored by thin-layer chromatography (TLC) on Yantai Wish chemical products Co., Ltd. (Yantai, China) silica gel 60F-254 by fluorescence quenching under UV light. All of the final compounds were purified by column chromatography. $^1\text{H-NMR}$ and $^{13}\text{C-NMR}$ spectra were recorded on an AV2 600 MHz spectrometer (Bruker Biospin, Swiss). Chemical shifts (δ) were given in parts per million (ppm) relative to tetramethylsilane (TMS) as an internal standard. Multiplicities were abbreviated as follows: single (s), doublet (d), doublet-doublet (dd), doublet-triplet (dt), triplet (t), triplet-triplet (tt), triplet-doublet (td), quartet (q), quartet-doublet (qd), multiplet (m), and broad signal (br s). Positive mode high-resolution mass spectral (HRMS) data were acquired using electrospray ionization (ESI) on a Q Exactive LC-MS/MS instrument (Thermo Fisher Scientific Inc., Waltham, MA, USA) with UV detection at 254 nm.

3.2. Synthesis of *N*-*o*-Tolylcycloadamantanecarboxamide (2)

A mixture of *o*-toluidine (10.0 mmol), adamantane-1-carbonyl chloride (10.0 mmol) and anhydrous potassium carbonate (7 mmol) in toluene (50 mL) was stirred at room temperature for 4 h. The resulting solids was filtered off and stirred at room temperature for 1.5 h with H_2O (50 mL). After completion of the reaction, the solid was filtered off and recrystallized from the appropriate solvent. White solid product, yield 75.5%. $^1\text{H-NMR}$ (CDCl_3): δ 7.88 (d, $J = 8.07$ Hz, 1H), 7.18–7.24 (m, 2H), 7.17 (d, $J = 7.52$ Hz, 1H), 7.05 (dt, $J = 1.10, 7.43$ Hz, 1H), 2.26 (s, 3H), 2.11 (br s, 3H), 1.99 (d, $J = 2.57$ Hz, 6H), 1.77 (q, $J = 12.29$ Hz, 6H). ESI-HRMS (+): m/z $[\text{M} + \text{H}]^+$ calculated for $\text{C}_{18}\text{H}_{23}\text{NO}^+$, 270.1852, found 270.1853; $[\text{M} + \text{Na}]^+$ calculated $\text{C}_{18}\text{H}_{23}\text{NONa}^+$, 292.1672, found 292.1669.

3.3. Synthesis of 2-Adamantane-1H-indole (3)

A stirred solution of compound 2 (10 mmol) in 50 mL of tetrahydrofuran (THF) under a N_2 atmosphere was maintained at an internal temperature of -5 to 5 $^\circ\text{C}$ and treated dropwise with 0.1–0.15 mol of 2.5 M *n*-BuLi in hexane. The mixture was stirred at ambient temperature for 3 h, cooled in an ice bath, and treated dropwise with 2 M HCl (12 mL). Then, the organic layer was separated and the aqueous layer washed with C_6H_6 . The combined organic layer was dried with anhydrous MgSO_4 , filtered, and concentrated *in vacuo*. The residue was recrystallized from the appropriate solvent. White solid product, yield 56.5%. $^1\text{H-NMR}$ (CDCl_3): δ 7.30 (d, $J = 7.89$ Hz, 1H), 7.18 (dd, $J = 0.55, 8.07$ Hz, 1H), 6.88 (dt, $J = 1.10, 7.52$ Hz, 1H), 6.77–6.83 (m, 1H), 5.98 (d, $J = 0.55$ Hz, 1H), 1.97 (d, $J = 2.57$ Hz, 3H), 1.93 (d, $J = 2.93$ Hz, 6H), 1.73 (br s, 6H). ESI-HRMS (+): m/z $[\text{M} + \text{H}]^+$ calculated for $\text{C}_{18}\text{H}_{21}\text{N}^+$, 252.1747, found 252.1748; $[\text{M} + \text{Na}]^+$ calculated for $\text{C}_{18}\text{H}_{21}\text{NNa}^+$, 274.1566, found 274.1568.

3.4. General Procedure for Synthesis of 5a–y [23,46]

A dry 50 mL capacity carousel reaction tube was charged with compound 3 (1.5 mmol), and this starting material was dissolved in dry ether (12 mL). Oxalyl chloride (1.65 mmol) was added and the mixture stirred at room temperature for 2 h, the solid was filtered off. Then compound 4 was used, without purification, for the next reaction. To a solution of 4 (1 mmol) and a substituted amine (1 mmol) in toluene (10 mL) was added K_2CO_3 (1.0 mmol), and the mixture stirred at room temp. After completion of the reaction, the mixture was concentrated and purified by column chromatography using appropriate mixtures of $\text{CH}_2\text{Cl}_2/\text{MeOH}$ to give compounds 5a–y.

N-Cyclopropyl-2-(2-adamantane-3H-indol-3-yl)-2-oxoacetamide (5a): yellow solid, yield 87.0%. $^1\text{H-NMR}$ ($\text{DMSO-}d_6$): δ 8.69 (d, $J = 4.58$ Hz, 1H), 7.53 (d, $J = 7.52$ Hz, 1H), 7.48 (d, $J = 7.52$ Hz, 1H), 7.24–7.27 (m, 1H), 2.89 (qt, $J = 3.97, 7.61$ Hz, 1H), 2.21 (br s, 6H), 2.08 (br s, 3H), 1.69–1.88 (m, 6H), 0.71–0.79 (m, 2H), 0.52–0.61 (m, 2H). $^{13}\text{C-NMR}$ ($\text{DMSO-}d_6$): δ 186.9, 170.3, 157.8, 134.7, 129.4, 122.3, 121.9, 119.8, 112.8,

108.2, 38.8, 36.5, 36.3, 28.3, 22.7, 21.5, 5.8. ESI-HRMS (+): m/z $[M + H]^+$ calculated for $C_{23}H_{26}N_2O_2^+$, 363.2067, found 363.2065; $[M + Na]^+$ calculated for $C_{23}H_{26}N_2O_2Na^+$, 385.1886 found 385.1888.

N-(4-Fluorobenzyl)-2-(2-adamantane-1H-indol-3-yl)-2-oxoacetamide (**5b**): yellow solid, yield 87.5%. 1H -NMR (DMSO- d_6): δ 9.17 (t, $J = 6.05$ Hz, 1H), 7.51 (d, $J = 8.07$ Hz, 1H), 7.42 (dd, $J = 5.69, 8.44$ Hz, 2H), 7.30 (d, $J = 8.07$ Hz, 1H), 7.18–7.23 (m, 2H), 7.09–7.13 (m, 1H), 6.92–6.96 (m, 1H), 4.46 (d, $J = 6.05$ Hz, 2H), 2.22 (br s, 6H), 2.07 (br s, 3H), 1.73–1.84 (m, 6H). ^{13}C -NMR (DMSO- d_6): δ 186.5, 169.2, 161.8 (d, $J = 243.2$ Hz), 158.4, 135.4 (d, $J = 3.3$ Hz), 130.3 (d, $J = 8.8$ Hz), 129.4, 128.4, 125.8, 121.9 (d, $J = 63.8$ Hz), 119.8, 115.6, 115.4, 112.9, 108.0, 41.6, 38.8, 36.6, 36.4, 28.4. ESI-HRMS (+): m/z $[M + H]^+$ calculated for $C_{27}H_{27}FN_2O_2^+$, 431.2129, found 431.2126; $[M + Na]^+$ calculated for $C_{27}H_{27}FN_2O_2 Na^+$, 453.1949, found 453.1949.

2-(2-Adamantane-1H-indol-3-yl)-2-oxo-*N*-(2-(pyridin-3-yl)ethyl)acetamide (**5c**): yellow solid, yield 86.0%. 1H -NMR (DMSO- d_6): δ 8.75 (t, $J = 5.41$ Hz, 1H), 8.53 (d, $J = 4.22$ Hz, 1H), 7.71 (dt, $J = 1.47, 7.61$ Hz, 1H), 7.51 (d, $J = 7.89$ Hz, 1H), 7.34 (t, $J = 8.16$ Hz, 2H), 7.24 (dd, $J = 5.23, 6.88$ Hz, 1H), 7.12 (t, $J = 7.43$ Hz, 1H), 7.04 (t, $J = 7.52$ Hz, 1H), 3.67 (q, $J = 6.97$ Hz, 2H), 3.00–3.06 (m, 2H), 2.20 (br s, 6H), 2.07 (br s, 3H), 1.72–1.84 (m, 6H). ^{13}C -NMR (DMSO- d_6): δ 187.1, 169.0, 158.4, 149.6, 136.9, 134.6, 127.9, 123.7, 122.2, 122.1, 121.9, 119.9, 112.7, 108.2, 40.0, 38.9, 38.7, 37.3, 36.5, 36.3, 28.4. ESI-HRMS (+): m/z $[M + H]^+$ calculated for $C_{27}H_{29}N_3O_2^+$, 428.2333, found 428.2330; $[M + Na]^+$ calculated for $C_{27}H_{29}N_3O_2Na^+$, 450.2152, found 450.2150.

2-(2-Adamantane-1H-indol-3-yl)-2-oxo-*N*-(2-(thiophen-2-yl)ethyl)acetamide (**5d**): yellow solid, yield 88.9%. 1H -NMR (DMSO- d_6): δ 11.69 (br s, 1H), 8.82 (t, $J = 5.50$ Hz, 1H), 7.51 (d, $J = 8.07$ Hz, 1H), 7.34–7.40 (m, 2H), 7.13 (t, $J = 7.52$ Hz, 1H), 7.04–7.09 (m, 1H), 6.97 (d, $J = 3.30$ Hz, 2H), 3.55 (q, $J = 6.85$ Hz, 2H), 3.05–3.13 (m, 2H), 2.21 (br s, 6H), 2.08 (br s, 3H), 1.73–1.83 (m, 6H). ^{13}C -NMR (DMSO- d_6): δ 167.1, 149.1, 137.8, 121.9, 114.7, 108.0, 107.6, 106.0, 104.7, 102.2, 100.1, 92.8, 88.4, 20.2, 19.0, 16.7, 16.5, 9.5, 8.5. ESI-HRMS (+): m/z $[M + H]^+$ calculated for $C_{26}H_{28}N_2O_2S^+$, 433.1944, found 433.1942; $[M + Na]^+$ calculated for $C_{26}H_{28}N_2O_2SNa^+$, 455.1764, found 455.1761.

N-(2-(1H-Indol-2-yl)ethyl)-2-(2-adamantane-1H-indol-3-yl)-2-oxoacetamide (**5e**): yellow solid, yield 87.9%. 1H -NMR (DMSO- d_6): δ 10.89 (brs, 1H), 8.79 (br s, 1H), 7.50–7.61 (m, 2H), 7.33–7.44 (m, 2H), 7.22–7.25 (m, 1H), 7.16–7.19 (m, 1H), 7.09 (dd, $J = 7.89, 16.14$ Hz, 2H), 6.97–7.01 (m, 2H), 3.59 (d, $J = 6.24$ Hz, 2H), 2.99 (t, $J = 7.15$ Hz, 2H), 2.22 (br s, 6H), 2.08 (br s, 3H), 1.70–1.85 (m, 6H). ^{13}C -NMR (DMSO- d_6): δ 187.3, 169.0, 157.6, 136.8, 129.4, 128.7, 127.9, 127.6, 125.8, 123.3, 122.2, 121.8, 121.4, 119.9, 118.7, 118.7, 112.7, 111.9, 41.6, 38.9, 36.6, 36.3, 28.4, 25.3. ESI-HRMS (+): m/z $[M + H]^+$ calculated for $C_{30}H_{31}N_3O_2^+$, 466.2489, found 466.2487; $[M + Na]^+$ calculated for $C_{30}H_{31}N_3O_2Na^+$, 488.2308, found 488.2306.

2-(2-Adamantane-3H-indol-3-yl)-2-oxo-*N*-phenylacetamide (**5f**): yellow solid, yield 91.9%. 1H -NMR (DMSO- d_6): δ 7.72–7.82 (m, 2H), 7.54 (d, $J = 8.07$ Hz, 1H), 7.35–7.44 (m, 3H), 7.15 (t, $J = 7.43$ Hz, 1H), 7.10 (t, $J = 7.52$ Hz, 1H), 6.97–7.03 (m, 2H), 6.56 (dd, $J = 1.10, 8.44$ Hz, 1H), 6.44–6.52 (m, 1H), 2.28 (br s, 6H), 2.10 (br s, 3H), 1.74–1.88 (m, 6H). ^{13}C -NMR (DMSO- d_6): δ 184.7, 167.9, 149.1, 139.1, 129.5, 129.2, 124.4, 122.0, 121.9, 120.2, 119.2, 116.1, 114.3, 107.7, 38.8, 36.6, 36.6, 28.4. ESI-HRMS (+): m/z $[M + H]^+$ calculated for $C_{26}H_{26}N_2O_2^+$, 399.2067, found 399.2063; $[M + Na]^+$ calculated for $C_{26}H_{26}N_2O_2Na^+$, 421.1886, found 421.1882.

2-(2-Adamantane-3H-indol-3-yl)-2-oxo-*N*-*p*-tolylacetamide (**5g**): yellow solid, yield 86.5%. 1H -NMR (DMSO- d_6): δ 10.68 (s, 1H), 7.66 (d, $J = 8.25$ Hz, 2H), 7.57 (d, $J = 8.07$ Hz, 1H), 7.41 (d, $J = 8.07$ Hz, 1H), 7.21 (d, $J = 8.25$ Hz, 2H), 7.14 (t, $J = 7.43$ Hz, 1H), 7.02–7.06 (m, 1H), 2.30 (s, 3H), 2.27 (br s, 6H), 2.11 (br s, 3H), 1.73–1.87 (m, 6H). ^{13}C -NMR (DMSO- d_6): δ 185.6, 167.4, 158.5, 136.4, 134.7, 133.6, 129.9, 129.4, 122.4, 122.2, 120.2, 119.4, 113.0, 107.9, 38.7, 36.5, 36.4, 28.4, 21.0. ESI-HRMS (+): m/z $[M + H]^+$

calculated for $C_{27}H_{28}N_2O_2^+$, 413.2224, found 413.2226; $[M + Na]^+$ calculated for $C_{27}H_{28}N_2O_2Na^+$, 435.2043, found 435.2045.

N-(2-Methoxyphenyl)-2-(2-adamantane-3H-indol-3-yl)-2-oxoacetamide (**5h**): yellow solid, yield 91.5%. 1H -NMR (DMSO- d_6): δ 9.44 (br s, 1H), 8.11 (d, $J = 7.70$ Hz, 1H), 7.44 (dd, $J = 8.07, 12.65$ Hz, 2H), 7.14–7.19 (m, 1H), 7.10 (d, $J = 8.07$ Hz, 1H), 7.00 (td, $J = 7.45, 19.03$ Hz, 2H), 6.91 (t, $J = 7.34$ Hz, 1H), 3.83 (s, 3H), 2.26 (br s, 6H), 2.06 (br s, 3H), 1.71–1.85 (m, 6H). ^{13}C -NMR (DMSO- d_6): δ 185.2, 168.0, 150.5, 130.1, 127.2, 125.4, 122.1, 121.0, 120.9, 120.8, 119.4, 114.7, 114.3, 111.9, 111.0, 107.6, 56.2, 39.2, 36.9, 36.9, 28.7. ESI-HRMS (+): m/z $[M + H]^+$ calculated for $C_{27}H_{28}N_2O_3^+$, 429.2173, found 429.2171; $[M + Na]^+$ calculated for $C_{27}H_{28}N_2O_3Na^+$, 451.1992, found 451.1990.

2-(2-Adamantane-3H-indol-3-yl)-2-oxo-*N*-(3-(trifluoromethyl)phenyl)acetamide (**5i**): yellow solid, yield 88.0%. 1H -NMR (DMSO- d_6): δ 8.22 (s, 1H), 8.02 (d, $J = 8.07$ Hz, 1H), 7.65 (t, $J = 7.98$ Hz, 1H), 7.51 (t, $J = 7.15$ Hz, 2H), 7.35 (d, $J = 8.07$ Hz, 1H), 7.23–7.27 (m, 1H), 7.17 (d, $J = 7.34$ Hz, 1H), 7.09 (t, $J = 7.52$ Hz, 1H), 6.98–7.02 (m, 1H), 2.27 (br s, 6H), 2.09 (br s, 3H), 1.73–1.86 (m, 6H). ^{13}C -NMR (DMSO- d_6): δ 183.8, 168.3, 140.0, 137.8, 130.8, 130.1 (d, $J = 31.9$ Hz), 129.4, 128.7, 125.8, 123.1 (q, $J = 280.6$ Hz), 119.0, 116.1 (q, $J = 3.3$ Hz), 113.8, 107.5, 38.8, 36.6, 28.4, 21.5. ESI-HRMS (+): m/z $[M + H]^+$ calculated for $C_{27}H_{25}F_3N_2O_2^+$, 467.1941, found 467.1943; $[M + Na]^+$ calculated for $C_{27}H_{25}F_3N_2O_2Na^+$, 489.1760, found 489.1762.

N-(4-Methoxyphenyl)-2-(2-adamantane-3H-indol-3-yl)-2-oxoacetamide (**5j**): yellow solid, yield 89.5%. 1H -NMR (DMSO- d_6): δ 10.60 (s, 1H), 7.68 (d, $J = 8.99$ Hz, 2H), 7.54 (d, $J = 7.89$ Hz, 1H), 7.41 (d, $J = 8.25$ Hz, 1H), 7.22–7.28 (m, 2H), 7.17 (d, $J = 7.34$ Hz, 2H), 7.10–7.16 (m, 2H), 7.01–7.07 (m, 1H), 6.97 (d, $J = 8.99$ Hz, 2H), 3.76 (s, 3H), 2.30 (s, 3H), 2.26 (br s, 6H), 2.10 (br s, 3H), 1.74–1.87 (m, 6H). ^{13}C -NMR (DMSO- d_6): δ 185.6, 167.9, 168.2, 158.6, 135.3, 134.7, 128.6, 127.1, 126.6, 122.3, 122.1, 119.5, 113.1, 107.9, 55.7, 38.7, 36.5, 36.5, 28.4, 19.05. ESI-HRMS (+): m/z $[M + H]^+$ calculated for $C_{27}H_{28}N_2O_3^+$, 429.2173, found 429.2168; $[M + Na]^+$ calculated for $C_{27}H_{28}N_2O_3Na^+$, 451.1992, found 451.1986.

N-(2,4-Dimethylphenyl)-2-(2-adamantane-1H-indol-3-yl)-2-oxoacetamide (**5k**): yellow solid, yield 81.5%. 1H -NMR (DMSO- d_6): δ 10.08 (br s, 1H), 7.55 (m, 2H), 7.38 (d, $J = 7.89$ Hz, 1H), 7.16 (t, $J = 7.34$ Hz, 1H), 7.11 (s, 1H), 7.09 (d, $J = 4.77$ Hz, 1H), 7.07 (s, 1H), 2.30 (s, 3H), 2.37 (s, 6H), 2.23 (s, 3H), 2.11 (s, 3H), 1.83 (m, 6H). ^{13}C -NMR (DMSO- d_6): δ 186.2, 167.9, 158.4, 135.5, 135.0, 133.0, 132.9, 131.6, 128.1, 127.2, 125.7, 122.3, 121.9, 119.7, 113.0, 108.0, 38.8, 36.6, 36.5, 28.4, 21.0, 18.1. ESI-HRMS (+): m/z $[M + H]^+$ calculated for $C_{28}H_{30}N_2O_2^+$, 427.238, found 427.2384; $[M + Na]^+$ calculated for $C_{28}H_{30}N_2O_2Na^+$, 449.2199, found 449.2201.

N-(4-Chloro-2-methylphenyl)-2-(2-adamantane-3H-indol-3-yl)-2-oxoacetamide (**5l**): yellow solid, yield 87.5%. 1H -NMR (DMSO- d_6): δ 7.56 (dd, $J = 8.25, 13.57$ Hz, 2H), 7.49 (d, $J = 8.07$ Hz, 1H), 7.39 (s, 1H), 7.34 (dd, $J = 2.02, 8.44$ Hz, 1H), 7.15 (t, $J = 7.61$ Hz, 1H), 7.08–7.11 (m, 1H), 2.26 (s, 9H), 2.10 (br s, 3H), 1.75–1.87 (m, 6H). ^{13}C -NMR (DMSO- d_6): δ 185.6, 167.9, 168.2, 158.6, 135.3, 134.7, 130.6, 128.6, 127.1, 126.6, 122.3, 122.1, 119.5, 113.1, 107.9, 38.7, 36.5, 36.5, 28.4, 19.05, 18.3. ESI-HRMS (+): m/z $[M + H]^+$ calculated for $C_{27}H_{27}ClN_2O_2^+$, 447.1834, found 447.1832; $[M + Na]^+$ calculated for $C_{27}H_{27}ClN_2O_2Na^+$, 469.1653, found 469.1649.

2-(2-Adamantane-3H-indol-3-yl)-*N*-(2-methyl-4-nitrophenyl)-2-oxoacetamide (**5m**): yellow solid, yield 90.5%. 1H -NMR (DMSO- d_6): δ 8.20 (brs, 1H), 8.17 (d, $J = 8.62$ Hz, 1H), 8.02 (d, $J = 7.70$ Hz, 1H), 7.56 (d, $J = 8.07$ Hz, 1H), 7.46 (d, $J = 8.07$ Hz, 1H), 7.16 (t, $J = 7.52$ Hz, 1H), 7.06–7.11 (m, 1H), 2.39 (s, 3H), 2.27 (br s, 6H), 2.10 (br s, 3H), 1.75–1.87 (m, 6H); ^{13}C -NMR (DMSO- d_6): δ 185.1, 168.2, 158.7, 144.3, 142.9, 134.8, 133.0, 127.9, 126.1, 124.6, 122.5, 122.4, 122.2, 119.4, 113.1, 107.9, 38.7, 36.5, 36.5, 28.4, 18.3. ESI-HRMS (+): m/z $[M + H]^+$ calculated for $C_{27}H_{27}N_3O_4^+$, 458.2074, found 458.2072; $[M + Na]^+$ calculated for $C_{27}H_{27}N_3O_4Na^+$, 480.1894, found 480.1892. methyl benzoate

Methyl 3-methyl-4-(2-(2-adamantane-3H-indol-3-yl)-2-oxoacetamido)benzoate (5n): yellow solid, yield 89.5%. $^1\text{H-NMR}$ (DMSO- d_6): δ 11.82 (s, 1H), 10.39 (s, 1H), 7.90 (s, 1H), 7.88 (d, $J = 1.65$ Hz, 1H), 7.82–7.87 (m, 1H), 7.56 (d, $J = 7.89$ Hz, 1H), 7.49 (d, $J = 8.07$ Hz, 1H), 7.12–7.16 (m, 1H), 7.08–7.12 (m, 1H), 3.86 (s, 3H), 2.34 (s, 3H), 2.24–2.29 (m, 6H), 2.11 (br s, 3H), 1.75–1.87 (m, 6H); $^{13}\text{C-NMR}$ (DMSO- d_6): δ 185.4, 167.8, 166.4, 158.5, 140.4, 134.7, 132.2, 132.0, 129.4, 128.7, 127.9, 126.8, 125.8, 124.7, 122.5, 122.2, 119.5, 113.0, 107.9, 52.5, 38.7, 36.5, 28.4, 21.5, 18.2. ESI-HRMS (+): m/z $[\text{M} + \text{H}]^+$ calculated for $\text{C}_{29}\text{H}_{30}\text{N}_2\text{O}_4^+$, 471.2278, found 471.2278; $[\text{M} + \text{Na}]^+$ calculated for $\text{C}_{29}\text{H}_{30}\text{N}_2\text{O}_4\text{Na}^+$, 493.2098, found 493.2096.

N-(3,4-Dimethoxyphenyl)-2-(2-adamantane-3H-indol-3-yl)-2-oxoacetamide (5o): yellow solid, yield 87.9%. $^1\text{H-NMR}$ (DMSO- d_6): δ 10.45 (br s, 1H), 7.49 (d, $J = 8.07$ Hz, 1H), 7.40 (d, $J = 2.38$ Hz, 1H), 7.35–7.37 (m, 1H), 7.05 (t, $J = 7.52$ Hz, 1H), 6.94–6.99 (m, 2H), 3.75 (d, $J = 8.25$ Hz, 6H), 2.27 (br s, 6H), 2.08 (br s, 3H), 1.72–1.86 (m, 6H). $^{13}\text{C-NMR}$ (DMSO- d_6): δ 167.7, 149.2, 145.8, 137.8, 132.8, 129.4, 128.7, 125.8, 121.6, 121.5, 111.9, 113.8, 112.7, 112.2, 107.7, 105.2, 56.2, 55.8, 39.6, 38.9, 36.7, 28.5. ESI-HRMS (+): m/z $[\text{M} + \text{H}]^+$ calculated for $\text{C}_{28}\text{H}_{30}\text{N}_2\text{O}_4^+$, 459.2278, found 459.2277; $[\text{M} + \text{Na}]^+$ calculated for $\text{C}_{28}\text{H}_{30}\text{N}_2\text{O}_4\text{Na}^+$, 481.2098, found 481.2098.

N-(3,5-Dimethoxyphenyl)-2-(2-adamantane-3H-indol-3-yl)-2-oxoacetamide (5p): yellow solid, yield 89.5%. $^1\text{H-NMR}$ (DMSO- d_6): δ 10.68 (s, 1H), 7.55 (d, $J = 8.07$ Hz, 1H), 7.39 (d, $J = 8.07$ Hz, 1H), 7.12–7.16 (m, 1H), 7.04–7.08 (m, 1H), 7.01 (s, 1H), 7.01 (s, 1H), 6.33 (t, $J = 2.20$ Hz, 1H), 3.74 (s, 6H), 2.26 (br s, 6H), 2.10 (br s, 3H), 1.74–1.86 (m, 6H). $^{13}\text{C-NMR}$ (DMSO- d_6): δ 185.3, 167.6, 161.1, 158.6, 140.6, 134.8, 129.4, 127.9, 122.4, 122.3, 119.4, 113.0, 107.8, 98.7, 96.2, 55.6, 38.7, 36.5, 36.5, 28.4. ESI-HRMS (+): m/z $[\text{M} + \text{H}]^+$ calculated for $\text{C}_{28}\text{H}_{30}\text{N}_2\text{O}_4^+$, 459.2278, found 459.2276; $[\text{M} + \text{Na}]^+$ calculated for $\text{C}_{28}\text{H}_{30}\text{N}_2\text{O}_4\text{Na}^+$, 481.2098, found 481.2096.

N-(4-Chloro-3-methoxyphenyl)-2-(2-adamantane-3H-indol-3-yl)-2-oxoacetamide (5q): yellow solid, yield 85.7%. $^1\text{H-NMR}$ (DMSO- d_6): δ 7.59 (s, 1H), 7.54 (d, $J = 7.89$ Hz, 1H), 7.43 (s, 2H), 7.38 (d, $J = 8.07$ Hz, 1H), 7.15–7.19 (m, 1H), 7.13 (t, $J = 7.70$ Hz, 1H), 7.02–7.07 (m, 1H), 3.79–3.88 (m, 3H), 2.26 (br s, 6H), 2.10 (br s, 3H), 1.74–1.86 (m, 6H). $^{13}\text{C-NMR}$ (DMSO- d_6): δ 184.8, 167.7, 155.1, 139.2, 137.8, 130.5, 129.0, 125.8, 122.2, 119.3, 116.3, 113.3, 112.9, 107.7, 104.8, 56.3, 40.1, 38.8, 36.6, 28.4, 21.5. ESI-HRMS (+): m/z $[\text{M} + \text{H}]^+$ calculated for $\text{C}_{27}\text{H}_{27}\text{ClN}_2\text{O}_3^+$, 463.1783, found 463.1781; $[\text{M} + \text{Na}]^+$ calculated for $\text{C}_{27}\text{H}_{27}\text{ClN}_2\text{O}_3\text{Na}^+$, 485.1602, found 485.1601.

N-(3-Chloro-4-fluorophenyl)-2-(2-adamantane-3H-indol-3-yl)-2-oxoacetamide (5r): yellow solid, yield 85.9%. $^1\text{H-NMR}$ (DMSO- d_6): δ 11.85 (br s, 1H), 11.01 (br s, 1H), 8.07 (dd, $J = 2.57, 6.79$ Hz, 1H), 7.68–7.72 (m, 1H), 7.56 (d, $J = 8.07$ Hz, 1H), 7.47 (t, $J = 9.08$ Hz, 1H), 7.36 (d, $J = 8.07$ Hz, 1H), 7.13–7.16 (m, 1H), 7.05–7.10 (m, 1H), 2.26 (br s, 6H), 2.10 (br s, 3H), 1.75–1.85 (m, 6H). $^{13}\text{C-NMR}$ (DMSO- d_6): δ 184.9, 167.4, 158.8 (d, $J = 244.3$ Hz), 154.1, 136.2, 134.7, 129.4, 128.7, 125.8, 122.5 (d, $J = 15.4$ Hz), 121.5, 120.6 (d, $J = 6.6$ Hz), 119.3, 117.8, 113.1, 107.7, 38.7, 36.5, 28.3, 21.5. ESI-HRMS (+): m/z $[\text{M} + \text{H}]^+$ calculated for $\text{C}_{26}\text{H}_{24}\text{ClFN}_2\text{O}_2^+$, 451.1583, found 451.1584; $[\text{M} + \text{Na}]^+$ calculated for $\text{C}_{26}\text{H}_{24}\text{ClFN}_2\text{O}_2\text{Na}^+$, 473.1403, found 473.1405.

N-(4-Bromo-2-fluorophenyl)-2-(2-adamantane-3H-indol-3-yl)-2-oxoacetamide (5s): yellow solid, yield 88.5%. $^1\text{H-NMR}$ (DMSO- d_6): δ 7.88 (br s, 1H), 7.68 (d, $J = 9.90$ Hz, 1H), 7.55 (d, $J = 8.07$ Hz, 1H), 7.43–7.52 (m, 2H), 7.14 (t, $J = 7.15$ Hz, 1H), 7.04–7.09 (m, 1H), 2.26 (br s, 6H), 2.10 (br s, 3H), 1.71–1.87 (m, 6H). $^{13}\text{C-NMR}$ (DMSO- d_6): δ 184.6, 168.0, 155.0 (d, $J = 249.8$ Hz), 129.4, 128.7, 128.2, 128.2, 128.1, 126.9, 125.8, 122.1 (d, $J = 29.7$ Hz), 119.8 (d, $J = 23.1$ Hz), 119.3, 113.2, 107.8, 38.7, 36.6, 36.5, 28.4. ESI-HRMS (+): m/z $[\text{M} + \text{H}]^+$ calculated for $\text{C}_{26}\text{H}_{24}\text{BrFN}_2\text{O}_2^+$, 495.1078, found 495.1079; $[\text{M} + \text{Na}]^+$ calculated for $\text{C}_{26}\text{H}_{24}\text{BrFN}_2\text{O}_2\text{Na}^+$, 517.0897, found 517.0896.

N-(5-Bromo-2-fluorophenyl)-2-(2-adamantane-3H-indol-3-yl)-2-oxoacetamide (5t): yellow solid, yield 85.6%. $^1\text{H-NMR}$ (DMSO- d_6): δ 8.17 (br s, 1H), 7.53 (d, $J = 8.07$ Hz, 1H), 7.46 (d, $J = 8.07$ Hz, 1H), 7.38 (br s,

1H), 7.30 (t, $J = 9.44$ Hz, 1H), 7.12 (t, $J = 7.24$ Hz, 1H), 7.03–7.08 (m, 1H), 2.25 (br s, 6H), 2.08 (br s, 3H), 1.74–1.85 (m, 6H). $^{13}\text{C-NMR}$ (DMSO- d_6): δ 170.3, 168.6, 154.1 (d, $J = 247.6$ Hz), 137.8, 129.4, 128.7, 128.2, 127.3, 125.8, 122.0 (d, $J = 28.6$ Hz), 119.4, 118.3 (d, $J = 21.0$ Hz), 116.2, 113.2, 107.9, 38.7, 36.6, 36.5, 28.4. ESI-HRMS (+): m/z $[\text{M} + \text{H}]^+$ calculated for $\text{C}_{26}\text{H}_{24}\text{BrFN}_2\text{O}_2^+$, 495.1078, found 495.1079; $[\text{M} + \text{Na}]^+$ calculated for $\text{C}_{26}\text{H}_{24}\text{BrFN}_2\text{O}_2\text{Na}^+$, 517.0897, found 517.0893.

N-(2-Fluoro-4-iodophenyl)-2-(2-adamantane-3H-indol-3-yl)-2-oxoacetamide (**5u**): yellow solid, yield 86.5%. $^1\text{H-NMR}$ (DMSO- d_6): δ 7.73 (d, $J = 9.72$ Hz, 2H), 7.61 (d, $J = 7.89$ Hz, 1H), 7.51 (d, $J = 7.89$ Hz, 1H), 7.45 (d, $J = 8.07$ Hz, 1H), 7.06–7.12 (m, 1H), 7.02 (t, $J = 7.43$ Hz, 1H), 2.26 (br s, 6H), 2.08 (br s, 3H), 1.74–1.86 (m, 6H). $^{13}\text{C-NMR}$ (DMSO- d_6): δ 170.3, 168.6, 154.9 (d, $J = 253.1$ Hz), 137.8, 134.0, 129.4, 128.7, 127.2, 125.8, 125.0 (d, $J = 22.0$ Hz), 121.7 (d, $J = 22.1$ Hz), 119.3, 113.6, 107.8, 38.8, 36.7, 36.6, 28.5. ESI-HRMS (+): m/z $[\text{M} + \text{H}]^+$ calculated for $\text{C}_{26}\text{H}_{24}\text{FIN}_2\text{O}_2^+$, 543.0939, found 543.0939; $[\text{M} + \text{Na}]^+$ calculated for $\text{C}_{26}\text{H}_{24}\text{FIN}_2\text{O}_2\text{Na}^+$, 565.0759, found 565.0757.

2-(2-Adamantane-3H-indol-3-yl)-2-oxo-*N*-(pyridin-3-yl)acetamide (**5v**): yellow solid, yield 88.6%. $^1\text{H-NMR}$ (DMSO- d_6): δ 11.93 (br s, 1H), 11.05 (s, 1H), 8.93 (d, $J = 2.02$ Hz, 1H), 8.38 (d, $J = 4.03$ Hz, 1H), 8.21 (d, $J = 8.25$ Hz, 1H), 7.59 (d, $J = 7.89$ Hz, 1H), 7.45 (dd, $J = 4.77, 8.07$ Hz, 1H), 7.39 (d, $J = 8.07$ Hz, 1H), 7.15 (t, $J = 7.61$ Hz, 1H), 7.04–7.09 (m, 1H), 2.27 (br s, 6H), 2.10 (br s, 3H), 1.74–1.86 (m, 6H). $^{13}\text{C-NMR}$ (DMSO- d_6): δ 185.0, 167.8, 158.8, 145.5, 141.8, 135.7, 134.8, 127.8, 127.3, 124.4, 122.5, 122.4, 119.3, 113.2, 107.7, 38.7, 36.5, 36.5, 28.3. ESI-HRMS (+): m/z $[\text{M} + \text{H}]^+$ calculated for $\text{C}_{25}\text{H}_{25}\text{N}_3\text{O}_2^+$, 400.202, found 400.2017; $[\text{M} + \text{Na}]^+$ calculated for $\text{C}_{25}\text{H}_{25}\text{N}_3\text{O}_2\text{Na}^+$, 422.1839, found 422.1836.

2-(2-Adamantane-3H-indol-3-yl)-2-oxo-*N*-(pyridin-2-yl)acetamide (**5w**): yellow solid, yield 90.6%. $^1\text{H-NMR}$ (DMSO- d_6): δ 11.93 (brs, 1H), 11.04 (s, 1H), 8.92 (d, $J = 2.20$ Hz, 1H), 8.38 (d, $J = 4.59$ Hz, 1H), 8.21 (d, $J = 8.25$ Hz, 1H), 7.59 (d, $J = 8.07$ Hz, 1H), 7.45 (dd, $J = 4.68, 8.16$ Hz, 1H), 7.39 (d, $J = 8.25$ Hz, 1H), 7.15 (t, $J = 7.61$ Hz, 1H), 7.04–7.09 (m, 1H), 2.27 (brs, 6H), 2.10 (brs, 3H), 1.74–1.87 (m, 6H). $^{13}\text{C-NMR}$ (DMSO- d_6): δ 185.0, 167.8, 158.8, 145.5, 141.8, 135.7, 134.8, 127.8, 127.3, 124.4, 122.5, 122.4, 119.3, 113.2, 107.7, 38.7, 36.5, 36.5, 28.3. ESI-HRMS (+): m/z $[\text{M} + \text{H}]^+$ calculated for $\text{C}_{25}\text{H}_{25}\text{N}_3\text{O}_2^+$, 400.202, found 400.2016; $[\text{M} + \text{Na}]^+$ calculated for $\text{C}_{25}\text{H}_{25}\text{N}_3\text{O}_2\text{Na}^+$, 422.1839, found 422.1835.

2-(2-Adamantane-3H-indol-3-yl)-2-oxo-*N*-(pyrimidin-5-yl)acetamide (**5x**): yellow solid, yield 90.1%. $^1\text{H-NMR}$ (DMSO- d_6): δ 9.16 (s, 2H), 8.97 (s, 1H), 7.54–7.59 (m, 1H), 7.38 (d, $J = 8.25$ Hz, 1H), 7.11–7.15 (m, 1H), 7.03–7.08 (m, 1H), 2.26 (br s, 6H), 2.09 (br s, 3H), 1.75–1.85 (m, 6H). $^{13}\text{C-NMR}$ (DMSO- d_6): δ 184.5, 168.2, 153.9, 148.4, 147.67, 129.3, 128.7, 128.1, 125.8, 122.3, 119.3, 113.4, 107.6, 38.7, 36.5, 36.5, 28.4, 19.1. ESI-HRMS (+): m/z $[\text{M} + \text{H}]^+$ calculated for $\text{C}_{24}\text{H}_{24}\text{N}_4\text{O}_2^+$, 401.1972, found 401.1969; $[\text{M} + \text{Na}]^+$ calculated for $\text{C}_{24}\text{H}_{24}\text{N}_4\text{O}_2\text{Na}^+$, 423.1791, found 423.1785.

N-(5-*tert*-Butylisoxazol-3-yl)-2-(2-adamantane-3H-indol-3-yl)-2-oxoacetamide (**5y**): yellow solid, yield 86.8%. $^1\text{H-NMR}$ (DMSO- d_6): δ 11.79 (br s, 2H), 7.56 (d, $J = 7.89$ Hz, 1H), 7.38 (d, $J = 8.07$ Hz, 1H), 7.16 (t, $J = 7.52$ Hz, 1H), 7.08–7.12 (m, 1H), 6.72 (s, 1H), 2.24 (br s, 6H), 2.10 (br s, 3H), 1.75–1.86 (m, 6H), 1.35 (s, 9H). $^{13}\text{C-NMR}$ (DMSO- d_6): δ 184.2, 181.5, 167.7, 158.9, 157.8, 134.8, 127.7, 122.7, 122.5, 122.4, 119.0, 113.2, 107.5, 99.8, 38.5, 36.5, 33.1, 28.9, 28.3. ESI-HRMS (+): m/z $[\text{M} + \text{H}]^+$ calculated for $\text{C}_{27}\text{H}_{31}\text{N}_3\text{O}_3^+$, 446.2438, found 446.2433; $[\text{M} + \text{Na}]^+$ calculated for $\text{C}_{27}\text{H}_{31}\text{N}_3\text{O}_3\text{Na}^+$, 468.2258, found 468.2256.

3.5. Cell Culture

All of the human cancer cell lines were obtained from the American Type Culture Collection (ATCC, Manassas, VA, USA) and grown in DMEM culture medium containing 10% fetal bovine serum (*v/v*) in 5% CO_2 at 37 °C.

3.6. Cytotoxicity against Cancer Cell Lines

Confluent cancer cells in good state were cultured in 96-well plates ($5-6 \times 10^3$ cells/well) and treated with various concentrations of compounds at 37 °C for 24 h. Then, the cells were incubated with 20 µL of 5 mg/mL 3-(4,5-dimethyl-2-thiazolyl)-2,5-diphenyl-2H-tetrazolium bromide, MTT, (Sigma-Aldrich, Saint Louis, MO, USA) reagent at 37 °C for 4 h. The supernatant was removed, and cells were dissolved in 150 µL dimethyl sulfoxide and shaken for 5 min. Finally, the light absorption (OD) of the dissolved cells was measured at 490 nm.

3.7. Western Blot Analysis

Equal amounts of the lysates were electrophoresed on 8% SDS-PAGE gel and transferred onto PVDF membranes (Roche, Shanghai, China). After blocked with 5% nonfat milk in TBST (20 mM Tris-HCl (pH 7.4), 150 mM NaCl and 0.1% Tween 20) for 1 h, The membranes were incubated with various primary antibodies overnight and secondary antibodies for 2 h, finally detected using ECL system. Proteins were detected with the following antibodies: Rabbit anti-Parp mAb (46D11, Cell Signaling Technology, Shanghai, China), Mouse anti-β-actin mAb (sc-8432, Santa Cruz, Shanghai, China).

3.8. A Flow Cytometry Assay

Hela cells were cultured in 6-well plate and treated with various compounds in serum free medium for 24 h. Then, the cells were detached by trypsin and fixed in 70% cold ethanol overnight at 4 °C. The next day, the cells were centrifuged in 3000 rpm for 53 min, washed twice in PBS, and incubated with DNase A (100 µg/mL) and propidium iodide (PI) solution (50 µg/mL) at room temperature for 30 min. The cell cycle was detected by flow cytometry (Beckman Coulter, Pasadena, CA, USA).

3.9. Colony Formation Assay

Hela cells were cultured in 6-well plate (200 cells/well) and treated with various compounds in 1% serum medium for 6 days. Then fixed with 4% paraformaldehyde and stained with 0.1% crystal violet.

3.10. Caspase Activity Assay

The activities of caspase-3, caspase-8 and caspase-9 were measured using the caspase activity kit (Beyotime Biotechnology, Shanghai, China) according to the manufacturer's instructions. Briefly, testis lysates were prepared after treatment. 50 µL testis lysate, 50 µL reaction buffer and 5 µL caspases substrate were added, incubated at 37 °C for 3 h. Samples were measured with an ELISA Reader (Bio-Rad instrument Group, Hercules, CA, USA) at an absorbance of 405 nm. All the experiments were carried out in triplicates.

4. Conclusions

In this paper, we synthesized and conducted a biological evaluation of a new series of *N*-substituted 2-(2-(adamantan-1-yl)-1*H*-indol-3-yl)-2-oxoacetamide derivatives as potential anticancer agents. The synthetic method was relatively simple, and the compounds were produced in high yields and easily purified. Compound **5r** showed more significant inhibitory activity against HepG2 cells than other compounds, with an IC₅₀ value of 10.56 ± 1.14 µM, as well as excellent selectivity toward HepG2 over HeLa and MCF-7 cells. Western blot analysis and flow cytometry assay demonstrated that compound **5r** could arrest the cell cycle, activate caspase-8 and caspase-3 and induce cell apoptosis. However, determining its roles in preventing cancer still require further intensive study.

Supplementary Materials: Supplementary materials can be accessed at: <http://www.mdpi.com/1420-3049/21/5/530/s1>.

Acknowledgments: This work was supported by the National Natural Science Foundation of China (No. 81273400, No. 81302652, No. 31471273 and 31461163002), the Project of South Center for Marine Research (14GYY023NF23). This research was also financially supported by Fujian Science and Technology project (Grant No.2014N5012) and the 10th Singapore-China Joint Research Program (S2014GR0448).

Author Contributions: H.H., F.W. and Y.Q. performed the synthesis and structure elucidation. X.Y., C.L. and J.Z. contributed in the biological activity. Z.W. and M.F. designed all molecules, prepared the manuscript and supervised whole research project.

Conflicts of Interest: The authors declare no conflict of interest.

References

1. Lozano, R.; Naghavi, M.; Foreman, K.; Lim, S.; Shibuya, K.; Aboyans, V.; Abraham, J.; Adair, T.; Aggarwal, R.; Ahn, S.Y.; *et al.* Global and regional mortality from 235 causes of death for 20 age groups in 1990 and 2010: A systematic analysis for the Global Burden of Disease Study 2010. *Lancet* **2013**, *380*, 2095–2128. [[CrossRef](#)]
2. Wilson, M.A.; Schuchter, L.M. Chemotherapy for Melanoma. In *Melanoma*; Springer: Cham, Switzerland, 2016; pp. 209–229.
3. Viaccoz, A.; Lekoubou, A.; Ducray, F. Chemotherapy in low-grade gliomas. *Curr. Opin. Oncol.* **2012**, *24*, 694–701. [[CrossRef](#)] [[PubMed](#)]
4. Venur, V.A.; Peereboom, D.M.; Ahluwalia, M.S. Current medical treatment of glioblastoma. *Springer Cancer Treat Res.* **2015**, *163*, 103–115.
5. Proctor, S.; Lennard, A.; Jackson, G.; Jones, G.; Lewis, J.; Wilkinson, J.; White, J.; Sieniawski, M.; McKay, P.; Culligan, D.; *et al.* The role of an all-oral chemotherapy containing lomustine (CCNU) in advanced, fs progressive Hodgkin lymphoma: A patient-friendly palliative option which can result in long-term disease control. *Ann. Oncol.* **2010**, *21*, 426–428. [[CrossRef](#)] [[PubMed](#)]
6. Rampling, R.; Sanson, M.; Gorlia, T.; Lacombe, D.; Lai, C.; Gharib, M.; Taal, W.; Stoffregen, C.; Decker, R.; van den Bent, M.J. A phase I study of LY317615 (enzastaurin) and temozolomide in patients with gliomas (EORTC trial 26054). *Neuro Oncol.* **2012**, *14*, 344–350. [[CrossRef](#)] [[PubMed](#)]
7. Szakács, G.; Paterson, J.K.; Ludwig, J.A.; Booth-Genthe, C.; Gottesman, M.M. Targeting multidrug resistance in cancer. *Nat. Rev. Drug Discov.* **2006**, *5*, 219–234. [[CrossRef](#)] [[PubMed](#)]
8. Gillet, J.-P.; Gottesman, M.M. Advances in the molecular detection of ABC transporters involved in multidrug resistance in cancer. *Curr. Pharm. Biotechnol.* **2011**, *12*, 686–692. [[CrossRef](#)] [[PubMed](#)]
9. Jemal, A.; Siegel, R.; Xu, J.Q.; Ward, E. Cancer Statistics, 2010. *Ca-Cancer J Clin.* **2010**, *60*, 277–300. [[CrossRef](#)] [[PubMed](#)]
10. Lal, S.; J Snape, T. 2-Arylindoles: A Privileged Molecular Scaffold with Potent, Broad-Ranging Pharmacological Activity. *Curr. Med. Chem.* **2012**, *19*, 4828–4837. [[CrossRef](#)] [[PubMed](#)]
11. Ding, S.; Dudley, E.; Plummer, S.; Tang, J.; Newton, R.P.; Brenton, A.G. Fingerprint profile of Ginkgo biloba nutritional supplements by LC/ESI-MS/MS. *Phytochemistry* **2008**, *69*, 1555–1564. [[CrossRef](#)] [[PubMed](#)]
12. Ahuja, P.; Siddiqui, N. Anticonvulsant evaluation of clubbed indole-1,2,4-triazine derivatives: A synthetic approach. *Eur. J. Med. Chem.* **2014**, *80*, 509–522. [[CrossRef](#)] [[PubMed](#)]
13. Zhang, M.-Z.; Mulholland, N.; Beattie, D.; Irwin, D.; Gu, Y.-C.; Chen, Q.; Yang, G.-F.; Clough, J. Synthesis and antifungal activity of 3-(1,3,4-oxadiazol-5-yl)-indoles and 3-(1,3,4-oxadiazol-5-yl)methyl-indoles. *Eur. J. Med. Chem.* **2013**, *63*, 22–32. [[CrossRef](#)] [[PubMed](#)]
14. Zhang, M.-Z.; Chen, Q.; Yang, G.-F. A review on recent developments of indole-containing antiviral agents. *Eur. J. Med. Chem.* **2015**, *89*, 421–441. [[CrossRef](#)] [[PubMed](#)]
15. Radwan, M.A.A.; Ragab, E.A.; Sabry, N.M.; El-Shenawy, S.M. Synthesis and biological evaluation of new 3-substituted indole derivatives as potential anti-inflammatory and analgesic agents. *Bioorg. Med. Chem.* **2007**, *15*, 3832–3841. [[CrossRef](#)] [[PubMed](#)]
16. Álvarez, R.; Puebla, P.; Díaz, J.F.; Bento, A.C.; García-Navas, R.; de la Iglesia-Vicente, J.; Mollinedo, F.; Andreu, J.M.; Medarde, M.; Peláez, R. Endowing Indole-Based Tubulin Inhibitors with an Anchor for Derivatization: Highly Potent 3-Substituted Indolephenstatins and Indoleisocombretastatins. *J. Med. Chem.* **2013**, *56*, 2813–2827. [[CrossRef](#)] [[PubMed](#)]

17. Carbone, A.; Parrino, B.; Vita, G.; Attanzio, A.; Spanò, V.; Montalbano, A.; Barraja, P.; Tesoriere, L.; Livrea, M.; Diana, P.; *et al.* Synthesis and Antiproliferative Activity of Thiazolyl-bis-pyrrolo[2,3-*b*]pyridines and Indolyl-thiazolyl-pyrrolo[2,3-*c*]pyridines, Nortopsentin Analogues. *Mar. Drugs* **2015**, *13*, 460–492. [[CrossRef](#)] [[PubMed](#)]
18. Carbone, A.; Pennati, M.; Barraja, P.; Montalbano, A.; Parrino, B.; Spanò, V.; Lopergolo, A.; Sbarra, S.; Doldi, V.; Zaffaroni, N.; *et al.* Synthesis and antiproliferative activity of substituted 3 [2-(1*H*-indol-3-yl)-1,3-thiazol-4-yl]-1*H*-pyrrolo[3,2-*b*]pyridines, marine alkaloid nortopsentin analogues. *Curr. Med. Chem.* **2014**, *21*, 1654–1666. [[CrossRef](#)] [[PubMed](#)]
19. Diana, P.; Carbone, A.; Barraja, P.; Montalbano, A.; Parrino, B.; Lopergolo, A.; Pennati, M.; Zaffaroni, N.; Cirrincione, G. Synthesis and Antitumor Activity of 3-(2-Phenyl-1,3-thiazol-4-yl)-1*H*-indoles and 3-(2-Phenyl-1,3-thiazol-4-yl)-1*H*-7-azaindoles. *Chemmedchem* **2011**, *6*, 1300–1309. [[CrossRef](#)] [[PubMed](#)]
20. Kuppens, I.E. Current state of the art of new tubulin inhibitors in the clinic. *Curr. Clin. Pharm.* **2006**, *1*, 57–70. [[CrossRef](#)]
21. Bacher, G.; Beckers, T.; Emig, P.; Klenner, T.; Kutscher, B.; Nickel, B. New small-molecule tubulin inhibitors. *Pure Appl. Chem.* **2001**, *73*, 1459–1464. [[CrossRef](#)]
22. Knaack, M.; Emig, P.; Bats, J.W.; Kiesel, M.; Müller, A.; Günther, E. Synthesis and Characterization of the Biologically Active 2-[1-(4-Chlorobenzyl)-1*H*-indol-3-yl]-2-oxo-*N*-pyridin-4-yl Acetamide. *Eur. J. Org. Chem.* **2001**, 3843–3847. [[CrossRef](#)]
23. Thompson, M.J.; Borsenberger, V.; Louth, J.C.; Judd, K.E.; Chen, B. Design, Synthesis, and Structure-Activity Relationship of Indole-3-glyoxylamide Libraries Possessing Highly Potent Activity in a Cell Line Model of Prion Disease. *J. Med. Chem.* **2009**, *52*, 7503–7511. [[CrossRef](#)] [[PubMed](#)]
24. Takhi, M.; Singh, G.; Murugan, C.; Thaplyyal, N.; Maitra, S.; Bhaskarreddy, K.; Amarnath, P.; Mallik, A.; Harisudan, T.; Trivedi, R.K.; *et al.* Novel and potent oxazolidinone antibacterials featuring 3-indolylglyoxamide substituents. *Bioorg. Med. Chem. Lett.* **2008**, *18*, 5150–5155. [[CrossRef](#)] [[PubMed](#)]
25. Lee, Y.-J.; Han, Y.-R.; Park, W.; Nam, S.-H.; Oh, K.-B.; Lee, H.-S. Synthetic analogs of indole-containing natural products as inhibitors of sortase A and isocitrate lyase. *Bioorg. Med. Chem. Lett.* **2010**, *20*, 6882–6885. [[CrossRef](#)] [[PubMed](#)]
26. Wang, T.; Yin, Z.; Zhang, Z.; Bender, J.A.; Yang, Z.; Johnson, G.; Yang, Z.; Zadjura, L.M.; D'Arienzo, C.J.; Parker, D.D.; *et al.* Inhibitors of Human Immunodeficiency Virus Type 1 (HIV-1) Attachment. 5. An Evolution from Indole to Azaindoles Leading to the Discovery of 1-(4-Benzoylpiperazin-1-yl)-2-(4,7-dimethoxy-1*H*-pyrrolo[2,3-*c*]pyridin-3-yl) ethane-1, 2-dione (BMS-488043), a Drug Candidate That Demonstrates Antiviral Activity in HIV-1-Infected Subjects. *J. Med. Chem.* **2009**, *52*, 7778–7787. [[PubMed](#)]
27. Taliani, S.; Trincavelli, M.L.; Cosimelli, B.; Laneri, S.; Severi, E.; Barresi, E.; Pugliesi, I.; Daniele, S.; Giacomelli, C.; Greco, G.; *et al.* Modulation of A2B adenosine receptor by 1-Benzyl-3-ketoindole derivatives. *Eur. J. Med. Chem.* **2013**, *69*, 331–337. [[CrossRef](#)] [[PubMed](#)]
28. Houlihan, W.J.; Parrino, V.A.; Uike, Y. Lithiation of *N*-(2-alkylphenyl)alkanamides and related compounds. A modified Madelung indole synthesis. *J. Org. Chem.* **1981**, *46*, 4511–4515. [[CrossRef](#)]
29. Robinson, M.W.; Overmeyer, J.H.; Young, A.M.; Erhardt, P.W.; Maltese, W.A. Synthesis and Evaluation of Indole-Based Chalcones as Inducers of Methuosis, a Novel Type of Nonapoptotic Cell Death. *J. Med. Chem.* **2012**, *55*, 1940–1956. [[CrossRef](#)] [[PubMed](#)]
30. Dominguez-Brauer, C.; Thu, K.L.; Mason, J.M.; Blaser, H.; Bray, M.R.; Mak, T.W. Targeting Mitosis in Cancer: Emerging Strategies. *Mol. Cell.* **2015**, *60*, 524–536. [[CrossRef](#)] [[PubMed](#)]
31. Weaver, B.A. How Taxol/paclitaxel kills cancer cells. *Mol. Biol. Cell.* **2014**, *25*, 2677–2681. [[CrossRef](#)] [[PubMed](#)]
32. Malumbres, M.; Barbacid, M. Cell cycle, CDKs and cancer: A changing paradigm. *Nat. Rev. Cancer* **2009**, *9*, 153–166. [[CrossRef](#)] [[PubMed](#)]
33. Malumbres, M. Physiological relevance of cell cycle kinases. *Physiol. Rev.* **2011**, *91*, 973–1007. [[CrossRef](#)] [[PubMed](#)]
34. Strebhardt, K. Multifaceted polo-like kinases: Drug targets and antitargets for cancer therapy. *Nat. Rev. Drug Discov.* **2010**, *9*, 643–660. [[CrossRef](#)] [[PubMed](#)]
35. Jacobson, M.D.; Weil, M.; Raff, M.C. Programmed cell death in animal development. *Cell* **1997**, *88*, 347–354. [[CrossRef](#)]

36. Mattson, M.P. Apoptosis in neurodegenerative disorders. *Nat. Rev. Mol. Cell Biol.* **2000**, *1*, 120–130. [[CrossRef](#)] [[PubMed](#)]
37. Kerr, J.F.; Winterford, C.M.; Harmon, B.V. Apoptosis. Its significance in cancer and cancer therapy. *Cancer* **1994**, *73*, 2013–2026. [[CrossRef](#)]
38. Eisenberg-Lerner, A.; Bialik, S.; Simon, H.; Kimchi, A. Life and death partners: Apoptosis, autophagy and the cross-talk between them. *Cell Death Differ.* **2009**, *16*, 966–975. [[CrossRef](#)] [[PubMed](#)]
39. Finckenberg, P.; Eriksson, O.; Baumann, M.; Merasto, S.; Lalowski, M.M.; Levijoki, J.; Haasio, K.; Kytö, V.; Muller, D.N.; Luft, F.C.; *et al.* Caloric restriction ameliorates angiotensin II-induced mitochondrial remodeling and cardiac hypertrophy. *Hypertension* **2012**, *59*, 76–84. [[CrossRef](#)] [[PubMed](#)]
40. Galluzzi, L.; Vitale, I.; Abrams, J.; Alnemri, E.; Baehrecke, E.; Blagosklonny, M.; Dawson, T.; Dawson, V.; El-Deiry, W.; Fulda, S.; *et al.* Molecular definitions of cell death subroutines: Recommendations of the Nomenclature Committee on Cell Death 2012. *Cell Death Differ.* **2012**, *19*, 107–120. [[CrossRef](#)] [[PubMed](#)]
41. Jin, Z.; El-Deiry, W.S. Overview of cell death signaling pathways. *Cancer Biol. Ther.* **2005**, *4*, 147–171. [[CrossRef](#)]
42. Oral, O.; Akkoc, Y.; Bayraktar, O.; Gozuacik, D. Physiological and pathological significance of the molecular cross-talk between autophagy and apoptosis. *Histol. Histopathol.* **2016**, *31*, 479–498.
43. Green, D.R.; Llamby, F. Cell Death Signaling. *Cold Spring Harbor Perspec. Biol.* **2015**, *7*. [[CrossRef](#)] [[PubMed](#)]
44. Lavrik, I.; Golks, A.; Krammer, P.H. Death receptor signaling. *J. Cell Sci.* **2005**, *118*, 265–267. [[CrossRef](#)] [[PubMed](#)]
45. Węsierska-Gądek, J.; Gueorguieva, M.; Wojciechowski, J.; Tudzarova-Trajkovska, S. *In vivo* activated caspase-3 cleaves PARP-1 in rat liver after administration of the hepatocarcinogen *N*-nitrosomorpholine (NNM) generating the 85 kDa fragment. *J. Cell Biochem.* **2004**, *93*, 774–787. [[CrossRef](#)] [[PubMed](#)]
46. Thompson, M.J.; Louth, J.C.; Ferrara, S.; Jackson, M.P.; Sorrell, F.J.; Cochrane, E.J.; Gever, J.; Baxendale, S.; Silber, B.M.; Roehl, H.H.; *et al.* Discovery of 6-substituted indole-3-glyoxylamides as lead antiprion agents with enhanced cell line activity, improved microsomal stability and low toxicity. *Eur. J. Med. Chem.* **2011**, *46*, 4125–4132. [[CrossRef](#)] [[PubMed](#)]

Sample Availability: Samples of all compounds are available from the authors.



© 2016 by the authors; licensee MDPI, Basel, Switzerland. This article is an open access article distributed under the terms and conditions of the Creative Commons Attribution (CC-BY) license (<http://creativecommons.org/licenses/by/4.0/>).